SANDIA REPORT

SAND2001-2585
Unlimited Release
Printed August 2001

Stereoscopic Height Estimation from Multiple Aspect Synthetic Aperture Radar Images

John M. DeLaurentis, and Armin W. Doerry

Prepared by
Sandia National Laboratories
Albuquerque, New Mexico 87185 and Livermore, California 94550

Sandia is a multiprogram laboratory operated by Sandia Corporation, a Lockheed Martin Company, for the United States Department of Energy under Contract DE-AC04-94AL85000.

Issued by Sandia National Laboratories, operated for the United States Department of Energy by Sandia Corporation.

Available to DOE and DOE contractors from
U.S. Department of Energy
Office of Scientific and Technical Information
P.O. Box 62
Oak Ridge, TN 37831

Telephone: (865)576-8401
Facsimile: (865)576-5728
E-Mail: reports@adonis.osti.gov
Online ordering: http://www.doe.gov/bridge

Available to the public from
U.S. Department of Commerce
National Technical Information Service
5285 Port Royal Rd
Springfield, VA 22161

Telephone: (800)553-6847
Facsimile: (703)605-6900
E-Mail: orders@ntis.fedworld.gov
Online order: http://www.ntis.gov/ordering.htm

SAND2001-2585
Unlimited Release
Printed August 2001

Stereoscopic Height Estimation from Multiple Aspect Synthetic Aperture Radar Images

John M. DeLaurentis
Computational Math/Algorithms Department

Armin W. Doerry
Synthetic Aperture Radar Department

Sandia National Laboratories
PO Box 5800
Albuquerque, NM 87185-0529

ABSTRACT

A Synthetic Aperture Radar (SAR) image is a two-dimensional projection of the radar reflectivity from a 3-dimensional object or scene. Stereoscopic SAR employs two SAR images from distinct flight paths that can be processed together to extract information of the third collapsed dimension (typically height) with some degree of accuracy. However, more than two SAR images of the same scene can similarly be processed to further improve height accuracy, and hence 3-dimensional position accuracy. This report shows how.

ACKNOWLEDGEMENTS

This work was funded by the US DOE Office of Nonproliferation & National Security, Office of Research and Development, under the Advanced Radar System (ARS) project. This effort is directed by Randy Bell of DOE NN-20.

CONTENTS

This page left intentionally blank.

1 Introduction

This report presents a stereoscopic method for reconstructing 3-dimensional information from multiple aspect Synthetic Aperture Radar (SAR) images. Although stereo SAR is not a new idea, the potential accuracy (as compared with IFSAR) and the possibility of using more than two aspect images have apparently been overlooked. Recently, the extent to which accurate and precise height estimates that can be made using stereo techniques has been clearly demonstrated for SAR images obtained from two distinct flight paths.[1] By considering stereoscopy as the trigonometric problem of determining the approximate intersection of several rays, we have extended the earlier stereo SAR work. This report describes the geometry for stereo SAR, presents a derivation of the approximate target location obtained from multiple aspect SAR images, and provides an expression for the error covariances.

2. Background

The basic SAR geometry is given in figure 1. In this schematic, the symbol $\mathbf{r}_{c0}$ denotes the vector from the Motion Compensation Point (MCP) to the Antenna Phase Center (APC_0) at the aperture phase center, **s** is the vector from the MCP to the target location and **m** is the vector from the universal coordinate frame center to the MCP. The target vector in the universal coordinate frame is given by **p=m+s**. The SAR image formation process, however, projects a target to a different apparent location at approximately $\mathbf{s}_{\text{¢}}=\mathbf{s}+s_z\mathbf{q}$ in the MCP reference frame, see figure 1. (A boldface variable denotes a vector.)

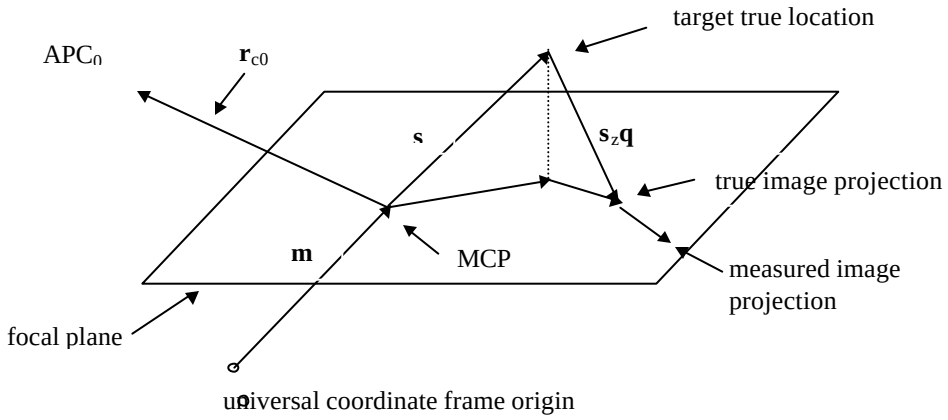

figure 1. Schematic of SAR Geometry

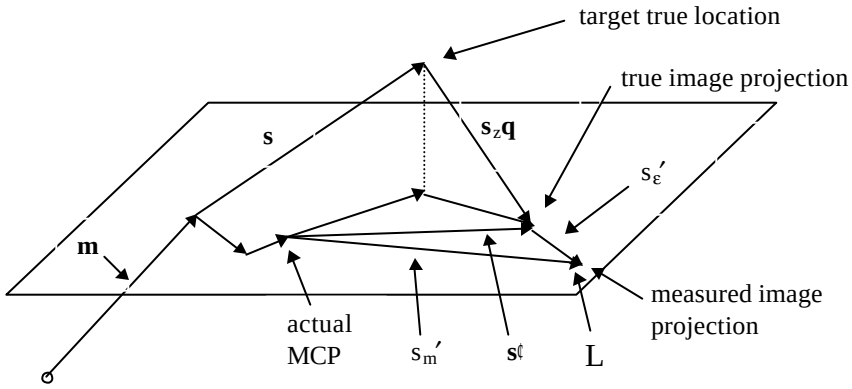

figure 2. Errors influencing target location

The vector **q**, which is normalized to a unit target height, identifies the displacement of the apparent target location from its true target location. That is, the vector $\mathbf{q}=(\mathbf{s}\text{¢}-\mathbf{s})/s_z$ describes the "layover" effect in SAR images, and is a function of the SAR data collection geometry.[1] For not-too-tall targets, especially near the scene center, **q** is approximately constant. It follows that **q** defines a line in space such that all targets, along the line, project to the same image point.

In practice, the measured image projection differs from the true projection. These errors arise from a variety of sources; a bias, $\mathbf{m}_b$, in the MCP position, random errors, $\mathbf{m}_\varepsilon$, in the MCP location, and a projection error, $\mathbf{s}_\varepsilon'$, see figure 2. In the universal coordinate frame, the measured MCP is given by $\mathbf{m}+\mathbf{m}_b+\mathbf{m}_\varepsilon$, and in the MCP reference frame, the measured image projection is given by $\mathbf{s}_m\text{¢}=\mathbf{s}\text{¢}+\mathbf{s}_\varepsilon$, see figure 2. The measured image projection in the universal reference frame, denoted **L**, may be written,

$$L=m+m_b+m_\varepsilon+s'+s_\varepsilon' , \qquad (1)$$

where $\mathbf{m}_\varepsilon$ and $\mathbf{s}_\varepsilon$ are mean zero random vectors (here and in the following we assume that the coordinate frame has been rotated to achieve an east-north–up alignment). Different image projections, **L**, and "layover" vectors, **q**, obtained from distinct flight trajectories constitute different aspect images, and can be used to estimate target location. If, in fact, all flight trajectories pass through the point APC_0, then distributed clutter in the SAR images will exhibit similar (in fact coherent) speckle patterns thereby allowing displacement measurements of the clutter, too.[2]

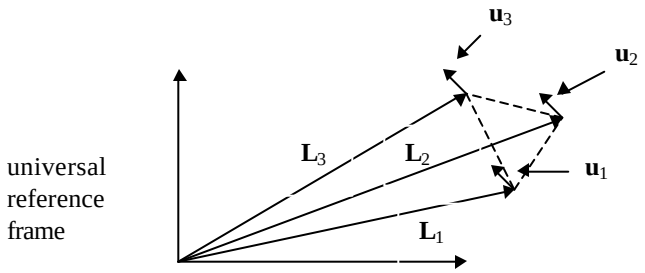

figure 3. Geometry for Stereo SAR

3. Multiple Aspect Stereo SAR

As mentioned in the preceding, the target may be located at any point (not too far from the focal plane) along the ray defined by the vector **q**, so the target location is not uniquely determined. One method for recovering the information needed to achieve uniqueness is called stereoscopy and usually involves the use of two pictures[3]; our technique applies to two or more images. The basic arrangement for three images is depicted in figure 3. The figure shows three image projections $\mathbf{L}_1$, $\mathbf{L}_2$, and $\mathbf{L}_3$, and three projecting unit vectors $\mathbf{u}_1$, $\mathbf{u}_2$, and $\mathbf{u}_3$. The unit vectors are taken in the opposite direction of the vectors $\mathbf{q}_i$, that is, $\mathbf{u} = -\mathbf{q}_i/|\mathbf{q}_i|$, and the projecting rays, ignoring measurement errors for the moment, would intersect at the true target location. Our method may be applied to n image projections $\mathbf{L}_i$, i=1,…,n, and n projecting unit vectors $\mathbf{u}_i$, i=1,…,n.

One approach is to find the best approximate location provided by every pair of projecting rays, and compute an average over these approximations, a more seamless approach, however, is to find the points that minimize the sum of the square of the distances separating all pairs of rays. Towards this end, we introduce the baseline vectors, for every pair (i,j) i<j,

$$b_{i,j}=L_j-L_i=m_j-m_i+m_{j,\varepsilon}-m_{i,\varepsilon}+s_j'-s_i'+s_{j,\varepsilon}'-s_{i,\varepsilon}', \tag{2}$$

where $\mathbf{L}_i=\mathbf{m}_i+\mathbf{m}_{i,b}+\mathbf{m}_{i,\varepsilon}+\mathbf{s}_i'+\mathbf{s}_{i,\varepsilon}$, and $\mathbf{m}_{i,b} = \mathbf{m}_{j,b}$, for all i and j, see equation (1). The ray emanating from the point $\mathbf{L}_i$ may be expressed as $\mathbf{y}_i=\mathbf{L}_i+x_i\mathbf{u}_i$, $0\le x_i<\infty$, and the square of the distance separating two rays is given by

$$\| (\mathbf{L}_i+x_i\mathbf{u}_i)-(\mathbf{L}_j+x_j\mathbf{u}_j)\|^2 = \|x_i\mathbf{u}_i-(\mathbf{b}_{i,j}+x_j\mathbf{u}_j)\|^2, \tag{3}$$

where $\|\mathbf{y}\|$ denotes the Euclidean norm of the vector $\mathbf{y}$, $\mathbf{y}\in R^n$, and i<j, see figure 3. The sum of the square of the distances between all pairs of rays is given by

$$J(\mathbf{x}) = \sum_{1\le i<j\le n} \| x_i\,\mathbf{u}_i - (\,\mathbf{b}_{i,j} + x_j\,\mathbf{u}_j)\|^2 . \tag{4}$$

Here, the sum is taken over all pairs (i,j) with $1\le i<j\le n$. We may rewrite expression (4) as

$$J(\mathbf{x})= \sum_{1\le i<j\le n} \|A_{i,j}\,\mathbf{x} - \mathbf{b}_{i,j}\|^2 , \tag{5}$$

where $\mathbf{x}\equiv(x_1,\ldots,x_n)^t$, $A_{i,j} \equiv [0,\ldots,0,\mathbf{u}_i,0,\ldots,-\mathbf{u}_j,0,\ldots,0]$, $\mathbf{0}=(0,\ldots,0)^t$, the superscript t denotes the transpose, and the brackets $[\mathbf{v}_1,\ldots,\mathbf{v}_n]$ designate a matrix with columns $\mathbf{v}_1,\ldots,\mathbf{v}_n$. The matrix $A_{i,j}$ has column vectors $\mathbf{0}$ for all columns except for the i^{th} and j^{th} columns, which are defined to be $\mathbf{u}_i$ and $-\mathbf{u}_j$ respectively.

A closed form for the minimum of expression (5) may be found by setting the gradient to zero,

$$\nabla J(\mathbf{x}) = 2 \sum_{1\le i<j\le n} A_{i,j}^{\,t} (A_{i,j}\,\mathbf{x} - \mathbf{b}_{i,j}). \tag{6}$$

Solving $\nabla J(\mathbf{x}) = 0$, we find a necessary condition for the minimum,

$$A\,\mathbf{x} = \mathbf{c}\,, \tag{7}$$

where $A = \sum_{1\le i<j\le n} A_{i,j}^t A_{i,j}$, and $\mathbf{c} = \sum_{1\le i<j\le n} A_{i,j}^t \mathbf{b}_{i,j}$. It can be shown that $J(\mathbf{x})$ is strictly convex, and if we assume that A is nonsingular then the unique global minimum is given by $\mathbf{x} = A^{-1}\,\mathbf{c}$. (We note that for the first pair of rays, if we set $J_1(\mathbf{x}) = \|A_{1,2}\,\mathbf{x} - \mathbf{b}_{1,2}\|^2$, so that $\nabla J_1(\mathbf{x}) = 2\,A_{1,2}^t\,(A_{1,2}\,\mathbf{x} - \mathbf{b}_{1,2})$; we obtain a necessary condition for minimizing $J_1(\mathbf{x})$, namely $A_{1,2}^t A_{1,2}\,\mathbf{x} = A_{1,2}^t\,\mathbf{b}_{1,2}$. It follows that equation (7) is a generalization of the case involving one pair of aspect images.)

The vector $\mathbf{x} = A^{-1}\,\mathbf{c}$ describes the set of points along the rays that minimize $J(\mathbf{x})$, but the rays most likely will not intersect. A natural recourse is to choose the average of these points as an estimate of the target location, namely,

$$\mathbf{y} = n^{-1} \sum_{1=i=n} \mathbf{y}_i = n^{-1} \sum_{1=i=n} (\mathbf{L}_i + x_i\,\mathbf{u}_i). \tag{8}$$

The vector $\mathbf{y}$ is an unbiased estimator for the location of the target, $\mathbf{p}$.

To show that $E\mathbf{y}$ equals the true target location we first compute the mean of the solution vector $\mathbf{x}$,

$$\bar{\mathbf{x}} = E\mathbf{x} = A^{-1}E\mathbf{c} = A^{-1}\bar{\mathbf{c}} \tag{9}$$

where $\bar{\mathbf{c}} = \sum_{1\le i<j\le n} E(A_{i,j}^t\,\mathbf{b}_{i,j}) = \sum_{1\le i<j\le n} A_{i,j}^t\,\mathbf{t}_{i,j}$, $\bar{\mathbf{x}} = (\bar{x}_1,\ldots,\bar{x}_n)$, $\mathbf{b}_{i,j} = \mathbf{t}_{i,j} + \mathbf{r}_{i,j}$, $\mathbf{t}_{i,j} = \mathbf{m}_j - \mathbf{m}_i + \mathbf{s}_j' - \mathbf{s}_i'$, $\mathbf{r}_{i,j} = \mathbf{m}_{j,\varepsilon} - \mathbf{m}_{i,\varepsilon} + \mathbf{s}_{j,\varepsilon}' - \mathbf{s}_{i,\varepsilon}'$, (see expression (2)), and $E\mathbf{r}_{i,j} = \mathbf{0}$. It follows that $\bar{\mathbf{x}}$ is the solution to equation (7) when no errors are present. Next, we derive an expression for the mean of $\mathbf{y}$,

$$E\mathbf{y} = n^{-1} \sum_{1=i=n} (\mathbf{L}_i + \bar{x}_i\,\mathbf{u}_i). \tag{10}$$

The vector $\bar{\mathbf{x}}$ minimizes $J(\mathbf{x})$ in the absence of errors; but, the minimum in this case occurs only when all the rays intersect at the target $\mathbf{p}$. It follows that $\mathbf{p} = \mathbf{L}_i + \bar{x}_i\,\mathbf{u}_i$ for all i, and $E\mathbf{y} = n^{-1} \sum_{1=i=n} (\mathbf{L}_i + \bar{x}_i\,\mathbf{u}_i) = n^{-1} \sum_{1=i=n} \mathbf{p} = \mathbf{p}$, as desired.

The covariance matrix of $\mathbf{y}$ may be derived from the covariance matrix for $\mathbf{x}$, setting $\mathbf{z} \equiv \mathbf{x} - \bar{\mathbf{x}} = A^{-1}\mathbf{c} - \bar{\mathbf{x}} = A^{-1}\sum_{1\le i<j\le n} A_{i,j}^t\,\mathbf{r}_{i,j}$ and $\Sigma \equiv E(\mathbf{z}\mathbf{z}^t)$, we have, from equations (8), (10),

$$\mathbf{y} - E\mathbf{y} = n^{-1} \sum_{1=i=n} \mathbf{u}_i\,(x_i - \bar{x}_i) = n^{-1} \sum_{1=i=n} \mathbf{u}_i z_i = n^{-1} U\mathbf{z} \quad . \tag{11}$$

where $U \equiv [\mathbf{u}_1,\ldots,\mathbf{u}_n]$. It follows that,

$$E[(\mathbf{y} - E\mathbf{y})(\mathbf{y} - E\mathbf{y})^t] = n^{-2}\,E\,[(U\mathbf{z})(U\mathbf{z})^t] = n^{-2}\,UE(\mathbf{z}\mathbf{z}^t)U^t = n^{-2}\,U\Sigma U^t\,. \tag{12}$$

Assuming that the entries of $U\Sigma U^t$ are of order n, it follows that the covariances are of order n^{-1}, in particular, the diagonal entries tend to zero, so the estimator $\mathbf{y}$ converges to $E\mathbf{y}$ in mean. Finally, since $E\mathbf{y} = \mathbf{p}$, we have arrived at the conclusion that $\mathbf{y}$ converges in mean to the true target location.

4. Summary & Conclusions

The preceding development clearly shows the following points.

- While stereo SAR utilizes two appropriately distinct SAR images to estimate target height, in fact more than two images (indeed an arbitrary number of multiple images) can be combined to improve the height estimate.
- Generally, more SAR images are better than fewer SAR images for better target height accuracy. The variance of the height estimate improves as the inverse of the number of images combined.
- Of course, better height accuracy also yields a better 3-D position accuracy.

References

1. Doerry, Armin, “High-precision stereoscopic 3-D mapping accuracy”, SPIE 2001 International Symposium on Aerospace/Defense Sensing, Simulation, and Controls, Algorithms for Synthetic Aperture Radar Imagery VIII, Vol. 4382, Orlando FL, 16 April 2001.

2. Jakowatz, Charles V. Jr., Daniel E. Wahl, Paul A. Thompson, “Three-Dimensional SAR Imaging Using Cross-Track Coherent Stereo Collections”, Conf. Record of the 31st Asilomar Conf. on Signals, Systems & Computers, Vol. 2, 1998.

3. Duda, R. O., and Hart, P. E., “Pattern Classification and Scene Analysis,” ISBN 0471223611, John Wiley & Sons, 1973.

DISTRIBUTION

Unlimited Release

1	MS 0509	M. W. Callahan	2300
1	MS 0529	B. C. Walker	2340
1	MS 0519	B. L. Burns	2340
1	MS 0537	R. M. Axline	2344
1	MS 0537	D. L. Bickel	2344
1	MS 0537	J. T. Cordaro	2344
1	MS 0537	W. H. Hensley	2344
1	MS 0529	K. W. Sorensen	2345
1	MS 0529	A. W. Doerry	2345
1	MS 0529	D. F. Dubbert	2345
1	MS 0529	S. S. Kawka	2345
1	MS 0529	M. S. Murray	2345
1	MS 0529	G. R. Sloan	2345
1	MS 0519	B. L. Remund	2348
1	MS 0519	S. D. Bensonhaver	2348
1	MS 0519	T. P. Bielek	2348
1	MS 0519	S. M. Devonshire	2348
1	MS 0519	J. A. Hollowell	2348
1	MS 0519	D. G. Thompson	2348
1	MS 0843	D. D. Boozer	15423
1	MS 1207	C. V. Jakowatz, Jr.	5912
1	MS 1207	N. E. Doren	5912
1	MS 1207	P. H. Eichel	5912
1	MS 1207	I. A. Erteza	5912
1	MS 1207	D. E. Wahl	5912
1	MS 0161	G. H. Libman	11500
1	MS 0328	F. M. Dickey	2612
1	MS 1110	D. E. Womble	9214
1	MS 1110	L. A. Romero	9214
1	MS 1100	J. M. Delaurentis	9214
1	MS 9018	Central Technical Files	8945-1
2	MS 0899	Technical Library	9616
1	MS 0612	Review & Approval Desk for DOE/OSTI	9612
1		Randy Bell	DOE NN-20